# $K$ X-Ray Yields of Primary $^{252}$Cf Fission Products

R. L. WATSON,* H. R. BOWMAN, AND S. G. THOMPSON
*Lawrence Radiation Laboratory, University of California, Berkeley, California*
(Received 8 May 1967)

The yields of $K$ x rays emitted by primary $^{252}$Cf fission products have been measured with a high-resolution [0.82 keV full width at half-maximum (FWHM) at 26.25 keV] lithium-drifted silicon spectrometer. The most noteworthy feature in the systematics of the observed x-ray yields is the presence of a pronounced even-odd fluctuation associated with the atomic numbers $Z=52$ through $Z=57$, in which the odd-$Z$-product x rays are found to be more intense than the even-$Z$-product x rays by approximately a factor of 2. This effect is not observed in the light-fission-product region. The x-ray yields observed in this experiment are compared with the results of previous experiments in which the $K$ x-ray yields were measured in association with the fission-fragment masses. Although general agreement is found in the over-all structural features, no evidence is seen in this study of the sudden drop in x-ray yield in the heavy-fission-product region corresponding to that which has previously been reported. The validity of the use of x-ray measurements as a method of determining the most probable charge distribution is examined in the light of the observed structure in the systematics of the x-ray yields.

## I. INTRODUCTION

SEVERAL recent investigations have resulted in measurements of the yields of $K$ x-rays and conversion electrons arising from the nuclear de-excitation of primary (pre-$\beta$-decay) fission products.[1–4] In these studies, the x-ray and electron yields were measured in association with the fragment masses and the resulting distributions have provided new information about the general features of nuclear structure in the fission-product region.

Other investigators have since studied the $K$ x rays arising from continuous sources of $^{235}$U fission fragments using high-resolution bent-crystal spectrometers.[5,6] These studies have resulted in accurate measurements of the various x-ray intensities. The systematics of these intensities reveal a number of interesting characteristics, including a pronounced even-odd effect in which the odd-$Z$ heavy-fragment x rays are found to be more intense than the even-$Z$ heavy-fragment x rays by approximately a factor of 2. Unfortunately, the extremely low efficiencies associated with bent-crystal spectrometers, in general, makes their use in a high-resolution coincidence-type experiment impractical.[7] Because of this limitation, the measurements of the above mentioned investigators include the contributions to the x-ray intensities of the $\beta$-decay products as well as the contributions of the primary products. Furthermore, because of absorption, it was not possible to measure the x-ray intensities associated with the light-fission products in these studies.

The continued improvement of semiconductor detectors, on the other hand, has finally led to resolution good enough to make their use in the measurement of x-ray intensities from complex mixtures of elements—such as those arising in fission—entirely feasible. This study was, therefore, undertaken with the purpose of measuring the intensities of *both* the light and heavy *primary* fission-product $K$ x rays by taking advantage of the suitability of semiconductor detectors for coincidence applications. The value of such a study stems from the fact that the results can be directly compared with the bent-crystal spectrometer measurements to shed additional light on the origin of the observed even-odd effect. In addition, a direct comparison can be made between this determination of primary $K$ x ray yield as a function of atomic number and the previous determinations of primary $K$ x-ray and conversion-electron yields as functions of mass.

## II. EXPERIMENTAL

A diagram of the experimental arrangement used is shown in Fig. 1. The x-ray energies were measured with a high-resolution lithium drifted silicon semiconductor spectrometer of dimensions 0.6 mm$^2\times$3 mm. The performance of this detector in the measurement of low-energy $\gamma$ rays and x rays is illustrated in Fig. 2, where it is seen that the energy resolution of the 26.25-keV line of $^{241}$Am was 0.82 keV full width at half-maximum (FWHM). A weightless source of $^{252}$Cf mounted on a 90-$\mu$g/cm$^2$ nickel foil and having a fission rate of $2.43\times10^5$ fissions per minute was separated from the x-ray spectrometer by 0.020 in. of beryllium and 0.002 in. of aluminum. Immediately behind the source was mounted a 0.05-cm-thick phosphorus-diffused silicon detector for counting fission fragments. The aluminum

* Present address: Department of Chemistry, Texas A&M University, College Station, Texas.

[1] L. E. Glendenin and J. P. Unik, Phys. Rev. **140**, B1301 (1965).
[2] S. S. Kapoor, H. R. Bowman, and S. G. Thompson, Phys. Rev. **140**, B1310 (1965). (Hereafter referred to as KBT.)
[3] R. A. Atneosen, T. D. Thomas, W. M. Gibson, and M. L. Perlman, Phys. Rev. **148**, 1206 (1966).
[4] R. L. Watson, Ph.D. thesis, University of California, Lawrence Radiation Laboratory Report No. UCRL-16798, 1966 (unpublished).
[5] J. E. Canty, C. D. Coryell, L. Leifer, and N. C. Rasmussen, Bull. Am. Phys. Soc. **10**, 481 (1965).
[6] W. John, R. Massey, and B. G. Saunders, Phys. Letters **24B**, 336 (1967).
[7] Acknowledgment is made of the bent-crystal–spectrometer studies of x rays coincident with the fission of $^{235}$U reported by B. W. Wehring and M. E. Wyman, Phys. Rev. (to be published).

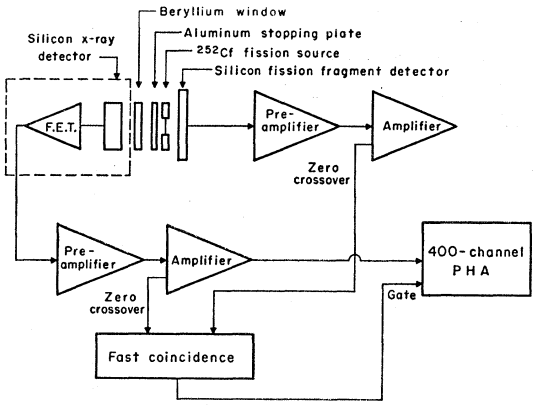


FIG. 1. A simplified diagram of the apparatus used to measure the energies of x rays from primary $^{252}$Cf fission products in coincidence with fission.

stopping plate and the fragment detector were located close enough to the fission source to insure that all fragments were stopped within $5\times10^{-11}$ sec after fission.

Timing pulses of the zero-crossover type were generated in the x-ray and fission-fragment amplifier systems and sent to a double-coincidence unit, where it was required that an x-ray be detected within the time interval of 0 to 93 nsec after fission in order to generate a gating signal. Whenever an event occurred in which the double-coincidence requirement was fulfilled, a gating signal was fed to a 400 channel pulse-height analyzer, which in turn analyzed the x-ray energy pulse. The accidental coincidence rate was measured by arbitrarily delaying the fission fragment timing pulses and was found to be less than 1% of the total coincidence rate.

It was very important to maintain an accurate energy calibration throughout the experiment. To avoid any possible calibration shifts, a digital gain stabilizer unit was incorporated into the electronic system and set to monitor the $K\alpha$ x ray peak of the cesium fission products throughout the run. A careful energy calibration was made before the experiment was started and checked again at the end. The calibration was achieved by measuring the $K$ x rays produced by fluorescent excitation of individual samples of all the elements throughout the fission-product region (Sr to Sm) for which a stable isotope exists. Examples of the x-ray distributions obtained using this procedure are shown in the bottom spectrum of Fig. 2. Each sample was fluoresced simultaneously with a cesium sample so as to produce cesium $K\alpha$ x rays upon which to stabilize. The 59.57 keV $\gamma$ ray of $^{241}$Am was used as the fluorescing source.

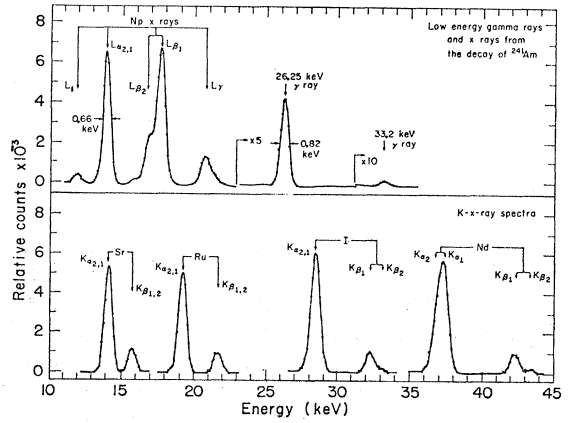


FIG. 2. X-ray and low-energy $\gamma$-ray spectra measured with a high resolution lithium-drifted silicon semiconductor spectrometer.

The x-ray spectrometer efficiency was calibrated by measuring the intensities of the 13.9-keV Np $L\alpha$ x rays, 17.8-keV Np $L\beta$ x rays, 20.8-keV Np $L\gamma$ x rays, 26.35-keV $\gamma$ ray, and 59.54-keV $\gamma$ ray arising from a calibrated source of $^{241}$Am (see top spectrum of Fig. 2) and of the 32.2-keV Ba $K\alpha$ x rays, and 36.4-keV Ba $K\beta$ x rays arising from a calibrated source of $^{137}$Cs.[8] The calibration sources were mounted in the same position as the fission source during the calibrations. The value of the efficiency times geometry reached a maximum ($\Omega\epsilon=2.46\times10^{-3}$) at an energy of 17.5 keV. The difference in x-ray absorption between the case of emission from fragments stopped in the aluminum plate and the case of emission from fragments stopped in the silicon fragment detector (an absorber thickness of approximately 5 mg/cm$^2$ Al+0.09 mg/cm$^2$ Ni+5 mg/cm$^2$ Si) was calculated to be negligible.

## III. ANALYSIS

The measured energy spectrum of $K$ x rays arising from primary $^{252}$Cf fission products is shown in Fig. 3. In this figure, the locations of the $K\alpha$ and $K\beta$ x-ray groups are indicated by brackets for various elements. Since the x-ray groups contributing to this spectrum were not fully resolved, it was necessary to resort to a

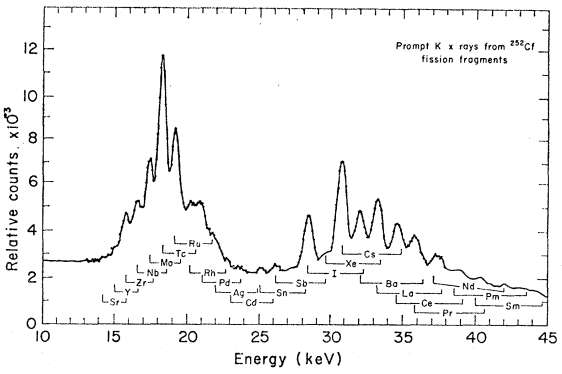


FIG. 3. The energy spectrum of $K$ x rays emitted by primary $^{252}$Cf fission products in coincidence with fission. The locations of the $K\alpha$ and $K\beta$ x-ray groups are indicated for most fission-product elements by brackets.

[8] Values of the relative intensities of these lines are given by C. M. Lederer, J. M. Hollander, and I. Perlman, *Table of Isotopes* (John Wiley & Sons, Inc., New York, 1967).

least-squares peak-fitting procedure in order to determine accurate values of the x-ray intensities for each element.

A computerized peak-fitting procedure was devised in which the four x-ray components comprising the $K$ x-ray group for a given element (i.e., the $K\alpha_2$, $K\alpha_1$, $K\beta_1$, and $K\beta_2$ components) were represented by four Gaussian functions. Each Gaussian function of every x-ray group was rigidly defined by specifying its first moment, standard deviation, and area relative to the area of the Gaussian function representing the $K\alpha_1$ x-ray component. A fit to the experimental data points was then achieved by varying, in combination, the areas of the various groups of Gaussian components utilizing the method of least squares. The fitting function used in the computer analysis was

$$f(x)=\sum_{k=1}^{n} N_k \sum_{l=1}^{m} R_{k,l}\frac{1}{(2\pi)^{1/2}\sigma_{k,l}} e^{-(x-\bar{x}_{k,l})^2/2\sigma_{k,l}^2}, \quad (1)$$

where

$N_k$ = the area of the Gaussian function representing the $K\alpha_1$ x-ray component belonging to group (element) $k$.

$R_{k,l}$ = the ratio of the areas of the $l$th x-ray component to the $K\alpha_1$ component for group (element) $k$.

$\sigma_{k,l}$ = the standard deviation of the $l$th Gaussian component belonging to group (element) $k$.

$\bar{x}_{k,l}$ = the first moment of the $l$th Gaussian component belonging to group (element) $k$.

The values of the parameters $\sigma_{k,l}$ and $\bar{x}_{k,l}$ were determined by making least-squares fits using Gaussian functions to the individual x-ray distributions obtained by fluorescing standard element samples during the energy calibration. In these fits, the intensities, first moments, and standard deviations were all allowed to vary so as to yield the best possible fit to the data. An example of how well the individual x-ray distributions could be fit using Gaussian functions is shown in Fig. 4. It was found that the x-ray distributions for elements

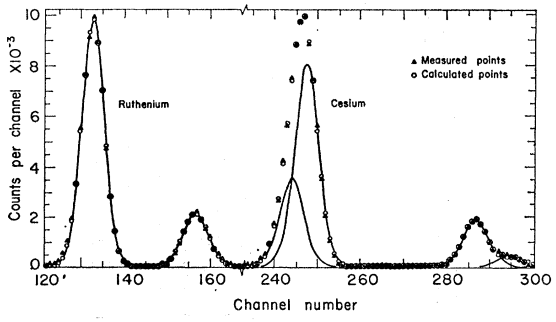


FIG. 4. $K$ x-ray distributions from flouresced samples of ruthenium and cesium showing the calculated distributions obtained by the method of least squares for the purpose of determining the parameters $\sigma_{k,l}$ and $\bar{x}_{k,l}$. The individual Gaussian fitting functions are shown by the solid curves.

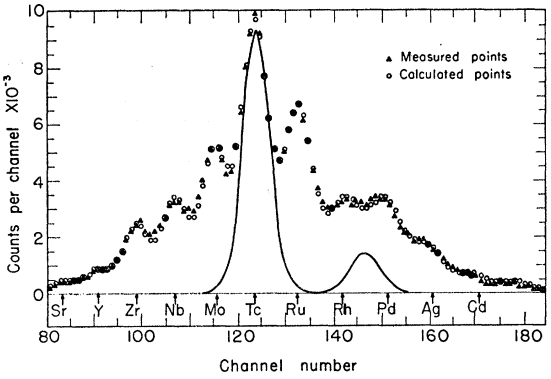


FIG. 5. The measured and calculated $K$ x-ray distributions associated with the primary light fission products (Sr to In) formed in the spontaneous fission of $^{252}$Cf. The Gaussian fitting functions for the element technetium are shown by the solid curves and the locations of the centroids of the $K\alpha$ x-ray groups belonging to the other elements are indicated by arrows.

below iodine could be represented quite well using only one Gaussian function for the $K\alpha_2$-$K\alpha_1$ components and one Gaussian function for the $K\beta_1$-$K\beta_2$ components (as is shown for the element ruthenium in Fig. 4). The energy spacings between the x-ray components for those elements above and including iodine, however, were large enough to require the use of individual Gaussian functions to represent each component. Hence, in the second summation of Eq. (1) the value of $m$ was 2 for fits to the light and intermediate fission-product x-ray distributions and 4 for fits to the heavy fission-product x-ray distributions. The values of $R_{k,l}$ used in Eq. (1) were those given by Wapstra *et al.*[9] The $R_{k,l}$ values for silver and barium were measured directly using sources of $^{109}$Cd and $^{137}$Cs and found to be in good agreement with the values given in Ref. 9.

The final fitted x-ray distribution associated with the light fission products (Sr to In) is shown in Fig. 5 and the fitted x-ray distribution associated with the heavy fission products (Sn through Sm) is shown in Fig. 6. As may be seen, the fits are quite good and the fact that only one variable parameter (namely $N_k$) was needed adds considerable confidence to the results.

## IV. RESULTS AND DISCUSSION

The yields of $K$ x rays *per fission* are shown in Fig. 7, plotted as a function of atomic number, and listed in Table I. Several noteworthy features are apparent; namely, (a) a pronounced even-odd fluctuation for atomic numbers 52 through 57, (b) a surprisingly low yield for xenon ($Z=54$), (c) a maximum in heavy-fission-product x-ray yield occurring at cesium ($Z=55$), and (d) a fairly smooth decrease in x-ray yield on either side of the maximum in the light-product x-ray yield, which occurs at technetium ($Z=43$). Hence, it is found

[9] A. H. Wapstra, G. J. Nijgh, and R. Van Lieshout, *Nuclear Spectroscopy Tables* (North-Holland Publishing Company, Amsterdam, 1959).

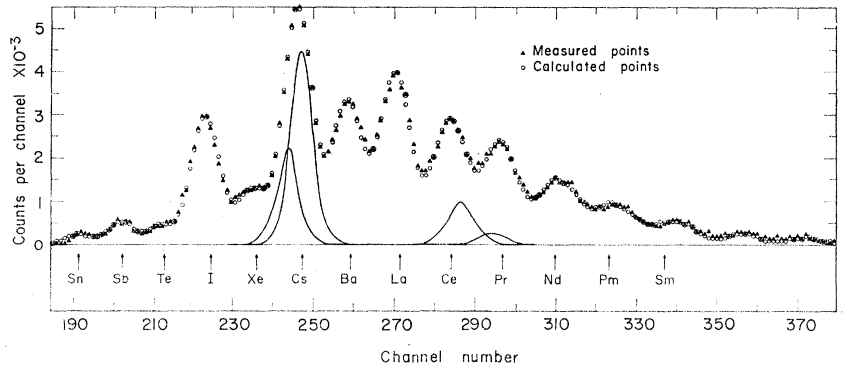


FIG. 6. The measured and calculated $K$ x-ray distributions associated with the primary heavy fission products (Sn to Sm) formed in the spontaneous fission of $^{252}$Cf. The Gaussian fitting functions for the element cesium are shown by the solid curves and the locations of the centroids of the $K\alpha_1$ x-ray components belonging to the other elements are indicated by arrows.

that two of the characteristics observed by John *et* al.[6] and Canty *et al.*[5] in the total (primary plus secondary) x-ray spectrum (i.e., the even-odd fluctuation and low xenon x-ray yield) are characteristic of the primary x-ray spectrum as well. It is noted, however, that the even-odd fluctuation arising from the primary fission products extends over a much more restricted region.

Comparison of the x-ray yields determined in this experiment with the results of Kapoor *et al.*[2] (referred to hereinafter as KBT) and of Glendenin and Griffin[1] provides a check on their accuracy. Summing the yields of all the light-fission-product, heavy-fission-product, and total-fission-product x rays gives values from this experiment of 0.205±0.005, 0.375±0.008, and 0.58 ±0.01 $K$ x rays *per fission*, respectively. The corresponding values given by KBT are 0.24±0.02, 0.32 ±0.02, and 0.56±0.04, and by Glendenin and Griffin are 0.16±0.02, 0.40±0.02, and 0.57±0.06. Hence, it is seen that the agreement is satisfactory.

In order to estimate the x-ray yields *per fragment*, the independent fission yield of each isotope formed in the spontaneous fission of $^{252}$Cf was calculated. Using the prescription given by Wahl *et al.*[10] in which the charge distribution of primary fission products is assumed to be Gaussian, the fractional independent yield of a fission product with charge $Z$ and mass $M$ is given by

$$Y_{I_M}{}^{(f)}(Z)=\frac{1}{(2\pi)^{1/2}\sigma}\int_{Z-\frac{1}{2}}^{Z+\frac{1}{2}} e^{-(Z_i-Z_p)^2/2\sigma^2}dZ_i, \quad (2)$$

where $Z_p$= the most probable charge for the mass chain of which the fission product is a member. $\sigma$= the standard deviation (width) of the charge distribution. Values of $Z_p$ used in these calculations were obtained from a curve derived from empirical $Z_p$ values given by Wahl *et al.*[10] and $Z_p$ values determined from x-ray measurements by KBT. The standard deviation of the Gaussian charge distribution was assumed to be constant and a value of $\sigma=0.59$ was used in the calculations

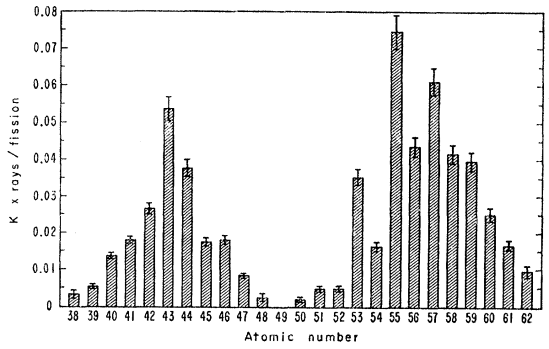


FIG. 7. The observed yields of $K$ x rays per fission arising from primary $^{252}$Cf fission products within 93 nsec after fission.

TABLE I. $K$ x-ray yields of primary $^{252}$Cf fission products.

| Element | ($K$ x rays)/fission |
|---|---|
| $_{38}$Sr | (0.33±0.10)×10$^{-2}$ |
| $_{39}$Y | (0.54±0.07)×10$^{-2}$ |
| $_{40}$Zr | (1.37±0.09)×10$^{-2}$ |
| $_{41}$Nb | (1.80±0.11)×10$^{-2}$ |
| $_{42}$Mo | (2.66±0.16)×10$^{-2}$ |
| $_{43}$Tc | (5.36±0.32)×10$^{-2}$ |
| $_{44}$Ru | (3.77±0.23)×10$^{-2}$ |
| $_{45}$Rh | (1.76±0.11)×10$^{-2}$ |
| $_{46}$Pd | (1.82±0.12)×10$^{-2}$ |
| $_{47}$Ag | (0.84±0.07)×10$^{-2}$ |
| $_{48}$Cd | (0.24±0.10)×10$^{-2}$ |
| $_{49}$In | <0.10×10$^{-2}$ |
| $_{50}$Sn | (0.18±0.07)×10$^{-2}$ |
| $_{51}$Sb | (0.48±0.07)×10$^{-2}$ |
| $_{52}$Te | (0.48±0.07)×10$^{-2}$ |
| $_{53}$I | (3.54±0.22)×10$^{-2}$ |
| $_{54}$Xe | (1.64±0.11)×10$^{-2}$ |
| $_{55}$Cs | (7.45±0.45)×10$^{-2}$ |
| $_{56}$Ba | (4.35±0.26)×10$^{-2}$ |
| $_{57}$La | (6.11±0.37)×10$^{-2}$ |
| $_{58}$Ce | (4.15±0.25)×10$^{-2}$ |
| $_{59}$Pr | (3.96±0.25)×10$^{-2}$ |
| $_{60}$Nd | (2.50±0.17)×10$^{-2}$ |
| $_{61}$Pm | (1.67±0.14)×10$^{-2}$ |
| $_{62}$Sm | (0.97±0.16)×10$^{-2}$ |

[10] A. C. Wahl, R. L. Ferguson, D. R. Nethaway, D. E. Troutner, and K. Wolfsberg, Phys. Rev. 126, 1112 (1962).

as given by Norris and Wahl.[11] Fission chain yields for $^{252}$Cf were obtained from the radiochemical measurements of Nervik.[12] By summing the calculated independent yields of all isotopes having the same atomic numbers over mass

$$Y(Z)=\sum_{M=1}^{n} Y_{IM}(Z); \qquad (3)$$

the element yields $Y(Z)$ were then computed and are tabulated in Table II. By dividing the x-ray yields *per fission* by these element yields, the x-ray yields *per fragment* were obtained and are shown in Fig. 8 plotted as a function of atomic number. The indicated errors in Fig. 8 reflect only the uncertainty in the x-ray intensity measurements and no attempt has been made to estimate the amount of error associated with the calculated element yields.

It is interesting to compare Fig. 8 with Fig. 9, taken from KBT, in which is plotted the $K$ x-ray yield per fragment versus fragment mass. For the most part, the general structural features are quite similar. Both figures exhibit sharp peaks in the light-fission-product regions with slight discontinuities to the right of the yield maxima, low yields in the vicinity of the doubly closed proton ($Z=50$) and neutron ($N=82$) shells, and a rather abrupt rise in yield in the heavy-fission-product region. One striking feature in Fig. 9 which seems to be missing in Fig. 8 is the sudden drop in yield to the right of the maximum yield in the heavy-fission-product region. In Fig. 9 it is seen that the sharp decrease in yield begins beyond mass 152. This mass is associated with a most probable charge of approximately 61, as is indicated on the scale along the top of Fig. 9. Moreover, the atomic number having the highest yield of mass 152 isotopes, as indicated by the top scale in Fig. 8, is calculated to be $Z=60$. One would expect, then, that a similar decrease in x-ray yield should occur for $Z\geq 61$. There appears to be no evidence of this in Fig. 8 and hence a definite difference between the results of the two types of experiments seems to exist. This difference, of course, could easily be due to error associated with the way in which the element yields used in the construction of Fig. 8 were calculated. On the other hand, since Figs. 8 and 9 represent plane views perpendicular to the $Z$ and $A$ axes, respectively, of a three-dimensional contour plot of x-ray yield versus $Z$ and $A$, the discrepancy between the two views might be an indication of a peculiar "$S$"-shaped bend in the heavy-fission-product x-ray-yield contours giving rise to a constant yield when summed along adjacent lines of constant $Z$ and decreasing yield when summed along

TABLE II. Calculated primary $^{252}$Cf fission-product-element yields.

| Light-product atomic number | Fission yield (%) | Heavy-product atomic number | Fission yield (%) | Average |
|---|---|---|---|---|
| 36 | 1.10 | 62 | 1.25 | 1.17 |
| 37 | 1.92 | 61 | 2.18 | 2.05 |
| 38 | 3.01 | 60 | 3.55 | 3.28 |
| 39 | 4.54 | 59 | 5.28 | 4.91 |
| 40 | 6.95 | 58 | 8.02 | 7.48 |
| 41 | 10.52 | 57 | 11.18 | 10.85 |
| 42 | 13.37 | 56 | 12.76 | 13.06 |
| 43 | 14.48 | 55 | 13.24 | 13.86 |
| 44 | 14.45 | 54 | 12.32 | 13.38 |
| 45 | 10.70 | 53 | 10.32 | 10.51 |
| 46 | 7.04 | 52 | 9.47 | 8.25 |
| 47 | 3.23 | 51 | 5.81 | 4.52 |
| 48 | 0.90 | 50 | 1.94 | 1.42 |
| 49 | 0.39 | 49 | 0.39 | 0.34 |

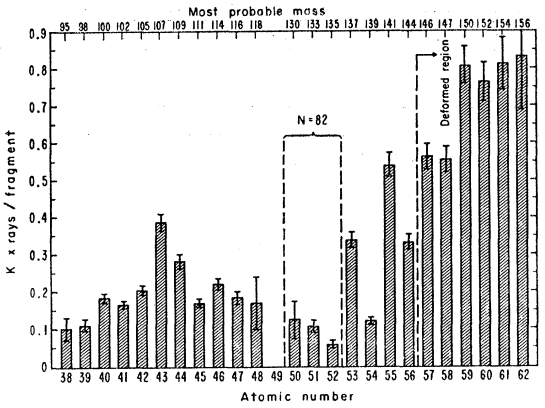


FIG. 8. Estimates of the yields of $K$ x rays per fragment arising from primary $^{252}$Cf fission products. The indicated errors reflect only the uncertainty in the x-ray intensity measurements. Atomic numbers for which $N=82$ closed-shell fission products are expected to occur are denoted and the approximate boundary of the deformed region is shown. The top scale indicates the calculated most-probable fragment mass associated with each atomic number.

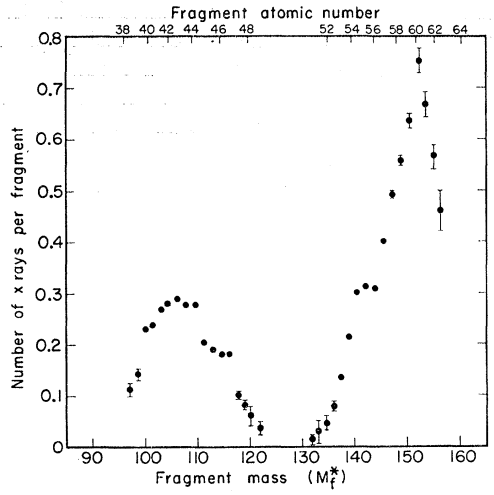


FIG. 9. The observed yields of $K$ x rays per fragment emitted within 50 nsec after fission from primary $^{252}$Cf fission products, versus the final masses ($M_f$*) of the fragments. The top scale indicates the average atomic number associated with each fragment mass (taken from Kapoor *et al.*, Ref. 2).

[11] Andrew E. Norris and Arthur C. Wahl, Phys. Rev. **146**, 926 (1966).

[12] W. E. Nervik, Phys. Rev. **119**, 1685 (1960).

adjacent lines of constant $A$. Still another alternative would be to accept the results of Fig. 8 as correct and ascribe the sharp decrease in yield observed in Fig. 9 to some sort of experimental error. Since this feature has been observed in at least three other independent studies of the same type, any error giving rise to this result would have to be common to all. The most likely source of error of this kind would probably be associated with the problem of relating x-ray yield to specific intervals of mass. In all of the experiments in which the x-ray yields were related to fragment mass, the masses of the fragments were calculated from measurements of their kinetic energies. These calculations, however, are unable to correct for neutron emission from the fragments except in an average way and hence considerable dispersion arises in the mass determinations. This dispersion can be expected to be largest for those fragments which emit, on the average, the greatest number of neutrons and has the effect of spreading any events being correlated with these masses over a broader distribution of adjacent mass intervals, thus resulting in a decrease in the observed total yield of events per mass interval. Results of previous studies[13] show that one of the regions of fragment mass associated with the emission of the greatest number of neutrons in the fission of $^{252}$Cf overlaps closely with the mass region in which the anomalous x-ray yield decrease is observed to occur in Fig. 9. The apparent discrepancy between Figs. 8 and 9 could, therefore, be an indication of the seriousness of this mass-dispersion effect.

Returning again to the even-odd fluctuation in the region extending from $Z=52$ to $Z=57$ in Fig. 8, it is not hard to explain this feature on the basis of known nuclear-structure systematics. It is reasonable, for example, to expect the variation of x-ray yield as a function of atomic number to reflect the relative importance of low-energy $\gamma$-ray transitions in the deexcitation processes of the various fission products, based upon the behavior of internal conversion coefficients as a function of transition energy. It follows, therefore, that low-energy transitions are more abundant for the odd-mass nuclei immediately to the right of the 50-proton–82-neutron doubly closed shell region than for even-mass nuclei in the same region. This is entirely consistent with the known systematics of even-mass spherical nuclei and the known systematics of odd-mass nuclei in this region. As the rare-earth deformed region is entered (the boundary of which is indicated approximately in Fig. 8), it is interesting to note that the even-odd fluctuation becomes washed out. This is most likely due to the increasingly important contributions to the even-$Z$ yields from low-energy $E$-2 rotational-type transitions in even-mass nuclides.

It should be pointed out, in the light of the observed alternation in x-ray yields for heavy fission products, that use of x-ray measurements in this region to determine the average fission-fragment charge for a given mass (i.e., the $Z_p$) may result in values which represent poorly the true charge distribution. It is important, for this technique to be applicable, that the internal conversion probability vary slowly and smoothly as a function of mass and charge. This, as has been shown, is definitely not the case. On the other hand, most of the error in these determinations will most likely be restricted to the even-mass chains since the x-ray fluctuations are probably most pronounced between adjacent even-even and odd-odd products. In fact, if the fluctuation between these pairs is fairly systematic, then the x-ray yield measurements may average out in such a way as to give $Z_p$ values which do not deviate appreciably from the true values after all. It is especially significant, in connection with these considerations, to note that in the data given by KBT, the largest deviations between the $Z_p$ values of complementary light and heavy fragments from a sum of 98 ($Z_{p_{lt}}+Z_{p_{hy}}=98$) occur for heavy fragment $Z_p$ values of 52.8, 55.4, and 56.1. The deviations for these values were 0.4, 0.4, and 0.3 units, respectively.

### ACKNOWLEDGMENTS

It is a pleasure to thank Mrs. Claudette Rugge for her work on the computer program used in the least-squares analyses, and Mrs. Joan Phillips for her help during the preparation of this manuscript.

[13] Harry R. Bowman, J. C. D. Milton, Stanley G. Thompson, and Wladyslaw J. Swiatecki, Phys. Rev. **129**, 2133 (1963).

# Erratum

**Theory of Proton-Proton Bremsstrahlung,** A. H. CROMER AND M. I. SOBEL [Phys. Rev. **152**, 1351 (1966)]. The sentence following Eq. (4.1) should read: "To sum over photon polarization we must integrate $d\phi/\pi$ from 0 to $2\pi$." The factor in front of the integral in Eq. (4.2) should be $\pi^{-1}$ instead of $(2\pi)^{-1}$. The factor of $\frac{1}{2}$ on the right-hand side of Eq. (4.5) should be omitted, together with the line immediately following.